

Review Article

Signaling mechanisms that direct cell fate specification and morphogenesis in human embryonic stem cells-based models of human gastrulation

 **Blerta Stringa** and  **Lilianna Solnica-Krezel**

Department of Developmental Biology and Center of Regenerative Medicine, Washington University School of Medicine in St. Louis, St. Louis, MO 63110, U.S.A.

Correspondence: Lilianna Solnica-Krezel (solnica@wustl.edu)

During mammalian gastrulation, a mass of pluripotent cells surrounded by extraembryonic tissues differentiates into germ layers, mesoderm, endoderm, and ectoderm. The three germ layers are then organized into a body plan with organ rudiments via morphogenetic gastrulation movements of emboly, epiboly, convergence, and extension. Emboly is the most conserved gastrulation movement, whereby mesodermal and endodermal progenitors undergo epithelial-to-mesenchymal transition (EMT) and move via a blastopore/primitive streak beneath the ectoderm. Decades of embryologic, genetic, and molecular studies in invertebrates and vertebrates, delineated a BMP > WNT > NODAL signaling cascade underlying mesoderm and endoderm specification. Advances have been made in the research animals in understanding the cellular and molecular mechanisms underlying gastrulation morphogenesis. In contrast, little is known about human gastrulation, which occurs *in utero* during the third week of gestation and its investigations face ethical and methodological limitations. This is changing with the unprecedented progress in modeling aspects of human development, using human pluripotent stem cells (hPSCs), including embryonic stem cells (hESC)-based embryo-like models (SCEMs). In one approach, hESCs of various pluripotency are aggregated to self-assemble into structures that resemble pre-implantation or post-implantation embryo-like structures that progress to early gastrulation, and some even reach segmentation and neurulation stages. Another approach entails coaxing hESCs with biochemical signals to generate germ layers and model aspects of gastrulation morphogenesis, such as EMT. Here, we review the recent advances in understanding signaling cascades that direct germ layers specification and the early stages of gastrulation morphogenesis in these models. We discuss outstanding questions, challenges, and opportunities for this promising area of developmental biology.

Introduction

Gastrulation is a fundamental developmental process in metazoans during which the three primary germ layers, ectoderm, mesoderm, and endoderm are induced and subsequently arranged into a body plan with organ rudiments. These germ layers will give rise to all the tissues and organs that contribute to animal physiology and neural functions, with ectoderm (EC) contributing to most of the neural tissues and skin epidermis, mesoderm (ME) forming cardiovascular and musculoskeletal systems, and definitive endoderm (DE) developing into the digestive system and lungs in some animals. Because human gastrulation is initiated at 14 days post fertilization (dpf) and occurs *in utero*, its experimental studies have been constrained by ethical concerns and technical limitations. Illuminating this understudied fundamental developmental process is of significant medical relevance because of a high

Received: 26 September 2023
 Revised: 22 November 2023
 Accepted: 24 November 2023

Version of Record published:
 12 December 2023

natural human embryo mortality, exceeding 50% of pregnancies, especially during the first weeks of conception [1,2]. Over the last decade, however, momentous inroads have been made by using human pluripotent stem cells (hPSCs), including human embryonic stem cells (hESCs) and human induced pluripotent stem cells (hiPSCs), to model aspects of human gastrulation in 2D and 3D culture systems. Insights from these *in vitro* models have to be verified with static histological studies such as the Carnegie Collection of Human Embryos, rare transcriptomic studies of human embryos at gastrulation stages (e.g. Carnegie Stage 7, CS7) [3], and *in vitro* cultured human embryos that initiate gastrulation [4,5]. Experimental studies of non-human primate gastrulae, including the cynomolgus monkey [6,7] and common marmoset [8], provide a valuable *in vivo* reference. Yet, our current understanding of the signaling events that induce, arrange, and shape the germ layers into a blueprint of the animal body comes from over 100 years of embryological, classical forward genetic, and molecular genetic studies in invertebrate animals such as the fruit fly, worm, sea urchin, tunicates, and vertebrate animals including frogs, fish, chick, and mouse [9–17]. In this review, we will focus on the recent advances in understanding signaling cascades that direct germ layers specification and gastrulation morphogenesis in human deduced from stem cell-based embryo models (SCEM) [18].

Setting up for gastrulation *in vivo*

Gastrulation in all animals is preceded by cell proliferation, activation of the zygotic genome, and the formation of a blastula (blastocyst in mammals), in which some cells remain pluripotent and some are specified as extra-embryonic. Specification of anteroposterior and dorsoventral polarity usually also precedes gastrulation [19]. In the case of mosaic development, early cell type specification and axis induction events are driven by maternally produced transcripts and proteins that are asymmetrically distributed in the egg and early embryo before the onset of zygotic transcription. In such mosaic development, often observed in invertebrate animals, but also in frogs and fish, blastomeres do not have equal potential and the zygotic genome is activated around the 1000-cell stage [20]. In contrast, mammalian embryogenesis exemplifies regulative development, whereby the early blastomeres retain pluripotency although some developmental biases may exist [21,22]. Regulative development is usually associated with early zygotic genome activation, which occurs at 2-cell stage in the mouse and 4–8-cell stage in human [23–25]. In these mammalian species, extraembryonic cell types are specified before implantation, resulting in a blastocyst that consists of an outer epithelial trophoblast (TE) that will give rise to the placenta and an inner cell mass (ICM) that comprises pluripotent cells within the pre-implantation epiblast (EPI) and primitive endoderm (PE) that separates the ICM from the blastocyst cavity (Figure 1A). The human blastocyst implants at 6–7 dpf (CS4) via the polar TE surrounding the ICM [2,25,26].

The post-implantation events from the ensuing week that precedes the onset of human gastrulation at 14 dpf (CS6.5) are known from histological studies of rare *in vivo* embryos [33] and from embryos fertilized and cultured *in vitro* without maternal tissues [34,35]. During this time the pluripotent and proliferating EPI is transformed into an epithelial vesicle (CS5). Its portion abutting the implanted polar TE acquires squamous epithelial morphology and forms amnion while the portion abutting the PE becomes a post-implantation EPI, from which all the germ layers (and some extraembryonic) cell types will arise (Figure 1A). This flat disc-shaped EPI of CS6a human and non-human primate embryos resembles the flat but significantly larger chick EPI [6,13]. However, it contrasts the cup-shaped murine EPI, which, at the onset of gastrulation (6 dpf), is surrounded by PE and the proximal edges of the murine EPI cup abut TE-derived extraembryonic ectoderm [26,36,37]. Of note, the zebrafish EPI (blastoderm) is also cup-shaped, but the inverted cup walls contain mesenchymal cells and it sits on top of a large syncytial yolk cell [38].

Gastrulation *in vivo* and its hESC-based models

As current ethical and technical barriers constrain the observation and experimentation of human embryos during gastrulation, stem-cell-based approaches are proving a valuable platform for modeling aspects of human gastrulation [39–42]. Several approaches have been devised based on the developmental properties of hESCs (Figure 1B). Conventional or primed hESCs were shown to be transcriptionally similar to cells from the EPI of human embryo at the onset of gastrulation and can be differentiated into the three germ layers and amnion, but not as efficiently into trophoblast and yolk sac derivatives [43]. Different culture conditions reprogram the primed hESCs into naïve hESCs that correspond to the blastocyst stage [44–46] and have the propensity to differentiate into the extraembryonic TE and PE [47–49]. Culture conditions have also been devised that support intermediate pluripotency states between ground and primed pluripotency [50]. In one approach, hESCs (of naïve, intermediate, or primed pluripotency) are aggregated and cultured in various media. Such 3D cultures,

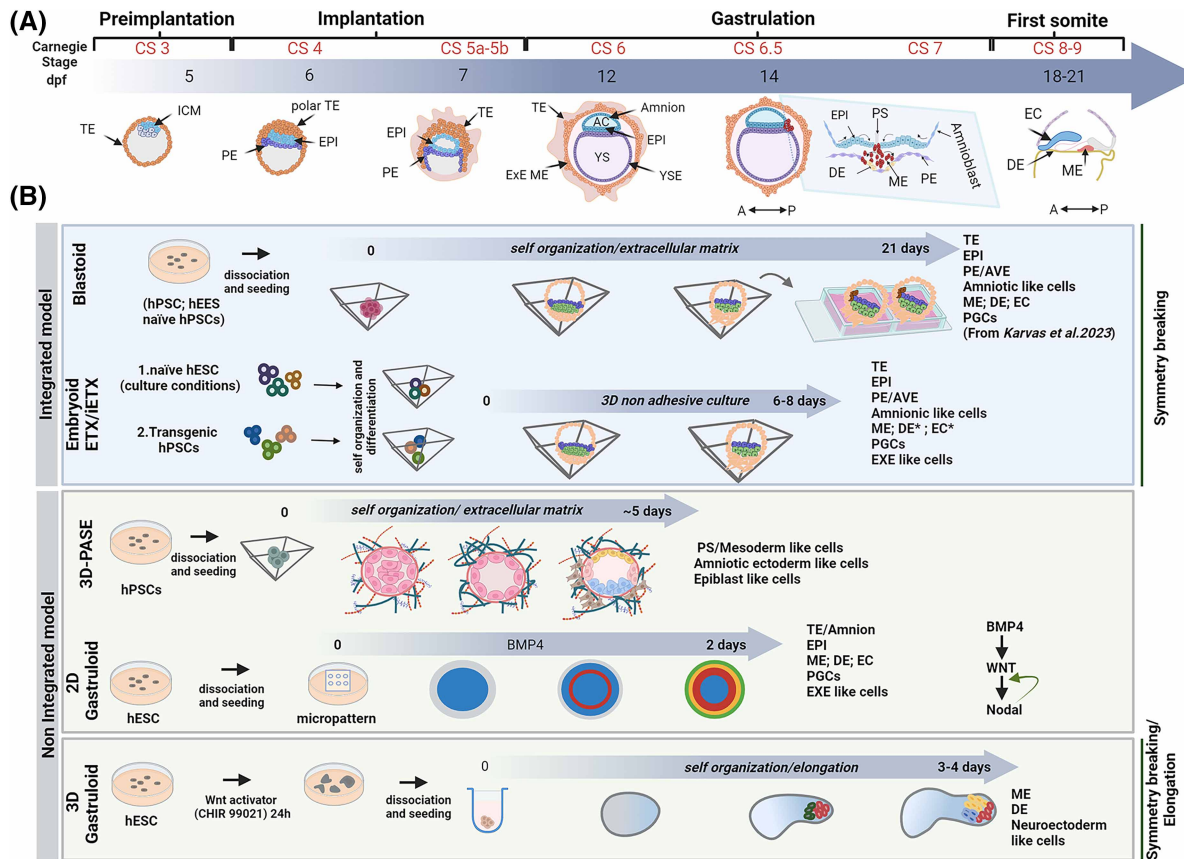


Figure 1. Stages of human embryogenesis *in vivo* and their *in vitro* stem cell-based embryo models (SCEMs).

(A) Schematic representation of human development from the blastocyst to the first somite stage at indicated Carnegie stages (CS) and corresponding days post fertilization (dpf). The blastocyst is formed ~5 dpf, and ~6 dpf, the inner cell mass (ICM) segregates into epiblast (EPI) and primitive endoderm (PE). Implantation into the uterine epithelium (not shown) via polar TE occurs around day 6–7. From day 12, the inner surface of the trophectoderm (TE) and the outer region of the amnion and yolk sac endoderm (YSE) become lined with extraembryonic mesoderm (ExE ME). At 14 dpf the primitive streak (PS) is evident, with superficial ectoderm (EC), and mesoderm (ME) and definitive endoderm (DE) undergoing epithelial to mesenchymal transition (EMT) and internalization. The miniature rectangle illustrates a transverse section of the PS with internalizing ME cells through EMT. **(B)** *In vitro* SCEMs generated using either, primed, naïve, or intermediate pluripotency hESCs. **Integrated models – Blastoid and Embryoid ETX/iETX model.** Each colored box contains a simplified description of the protocol for the representative models. Blastoids can be generated from primed hPSC or naïve hPSCs and arise by self-organization but only the illustrated model from naïve hESCs cultured for 21 days shows EMT and symmetry breaking (documented cell types shown on the right) [27]. Embryoid ETX/iETX models from (1) Oldak et al. [28], and (2) Weatherbee et al. [29] originate from different cell types. Transgenic approaches or/and specific culture conditions are used to generate TE, PE and EPI cells that are aggregated and assemble by day 8 in peri-gastrulation SCEMs (as described on the right). Differences and similarities in the protocols contribute to models that bypass the pre-implantation stages and achieve significant features of post-implantation development. **Non-integrated models.** Primed hESCs or hPSCs relying on endogenous or exogenous signaling direct differentiation in these models. 3D-PASE simulates the development of human amniotic sac and ME/PS formation with features of EMT and cell migration. In 2D micropatterned gastruloid exogenous BMP signaling initiates waves of BMP, WNT and NODAL signaling activity to induce germ layers, PS and EMT behaviors [30,31]. 3D gastruloid model generated by stimulation of WNT signaling in aggregated hESCs leads to ME, EC and DE specification, symmetry breaking in the absence of extraembryonic cells and elongation [32]. AC, amniotic cavity; AVE, anterior visceral endoderm; HPGCLs, human primordial germ cells like cells; YS, yolk sac; (**) [28].

or stem cell-based embryo models (SCEMs) [18], exhibit remarkable potential for self-assembly and self-patterning, developing into structures that reach pre- and post-implantation blastocyst stages with various contributions of EPI, TE, PE, and/or amnion, even exhibiting features of early gastrulation [27,51,52]. Another methodology entails combining peri-implantation-like pluripotent hESCs with hESCs expressing transgenes to promote either TE or PE fate into aggregates that self-assemble *in vitro* into post-implantation blastocysts and progress *in vitro* up to early gastrulation stages [29]. Alternatively, TE and PE fates are achieved by coaxing naïve hESCs with specific culture conditions and aggregating them with primed hESCs to generate SCEMs reaching early gastrulation [28]. In a yet different approach to modeling aspects of gastrulation by bypassing pre- and post-implantation stages, primed hESCs are cultured on 2D micropatterned discs and treated with BMP4, resulting in 2D gastruloids with concentric rings of extraembryonic, definitive endoderm (DE), mesoderm (ME), and ectoderm (EC) cells in the center [30]. Finally, aggregates of primed hESCs treated with WNT signaling agonists differentiate into elongating 3D gastruloids that feature three germ layers without extraembryonic cell types [32] (Figure 1B; Table 1). The constructs that model pre- and/or post-implantation stages and formation of both embryonic and extraembryonic cell types, are referred to as integrated models, contrasting non-integrated models, usually generated from primed hESCs, like 2D- and 3D-gastruloids that model development of germ layers largely without extraembryonic lineages (Figure 1B) [53]. Below we will discuss the mechanisms of germ layer induction and morphogenesis delineated by experimental studies of research organisms *in vivo* and the insights into these processes from different embryo models, their current limitations, outstanding questions, and opportunities.

Induction of mesendoderm precursors and anteroposterior embryonic polarity *in vivo*

The murine EPI appears to be symmetric until the first morphogenetic movement of embryo is initiated in what will become the posterior of the EPI and future embryo [36]. However, gene expression analyses in the mouse embryo reveal that germ layer specification has already been initiated at 6 dpf with transcripts of *Tbxt* in ME precursors detected in the proximal posterior EPI, marking the primitive streak (PS) [36,56]. The signaling cascade that induces ME and DE precursors and thus specifies the anteroposterior embryonic axis in mammals is best understood in the mouse [17]. At the top of the cascade is BMP signaling, with BMP4 ligands emanating from the extraembryonic ectoderm to induce *Wnt3* expression in the proximal primitive endoderm and epiblast [57] and being required for mesoderm formation [58]. *Wnt* signaling in turn induces expression of another TGF- β family member, *Nodal*. Whereas BMP4 is expressed in the entire extraembryonic ectoderm and signals to the entire proximal EPI [59], the BMP, *Wnt*, and *Nodal* signaling activity is limited to the prospective posterior EPI via antagonists of these pathways (*Dkk*, *Lefty*, *Cerberus*) secreted by the Anterior Visceral Endoderm (AVE). The AVE is a specialized PE population that moves asymmetrically from the distal EPI position proximally, thus defining future anteroposterior polarity and limiting mesendoderm induction and PS formation to the posterior EPI (reviewed in [37]). During gastrulation, the PS extends anteriorly/distally as different ME and DE cell types undergo EMT and internalization with its anterior tip becoming an evolutionarily conserved signaling center, Spemann–Mangold organizer [60]. The organizer gives rise to axial mesoderm (prechordal plate and notochord) and secretes *Wnt* and BMP antagonists and *Nodal* ligands to pattern the nascent germ layers and gastrulation movements [61].

Studies of non-human primates and *in vitro* cultured human embryos point to the ME inducing signal as BMP4 ligands secreted by amnion [8,62]. Notably, a putative AVE-like signaling center in the PE underlying the EPI has been identified, expressing BMP, NODAL, and FGF antagonists, including *CER1*, *LEFTY1*, *LEFTY2*, and *SHISA2* [63]. The asymmetric expression of these genes in the PE implies an AVE-like activity that would limit ME induction to the posterior region of the epiblast thus defining the anteroposterior embryonic axis.

Modeling induction of mesendoderm and embryonic polarity in SCEMs

The current SCEMs recapitulate to various degrees symmetry breaking-like events and ME, DE, and PS formation. Several embryo models have been generated from naïve hPSCs derived in either PXGL [45,64] or 5i/L/A culture conditions [44]. In aggregation culture, these naïve hPSCs self-organize into fluid-filled vesicular structures composed of TE-, PE- and ICM-like cell types and resembling natural human blastocysts at pre- and peri-implantation stages, hence dubbed blastoids, which were initially generated by combining murine ESC and TE cells [65]. The current models vary in efficiency of blastoid formation, cellular composition, and are limited in

Table 1. Comparison of the cell type of origin, cellular, and tissue composition of the described SCEMs

Developmental stage	Model	Cell of origin	Self organization vs exogenous signals	Signaling underlying ME specification	Cellular composition							Gastrulation patterning and morphogenetic events		References	
					Germ layers			Other cell types				AP symmetry breaking	ME cell EMT migration		
					ME	DE	EC	HPGC-like	Amnion	TE	PE/hypoblast				
Pre-implantation blastoids (from 5 dpf)	Blastoid	Naïve hPSCs	Self organization		YES	YES	YES	YES	YES	YES	YES	YES	NO	[27]	
		hEEs	Self organization	BMP → WNT → NODAL	YES	NO	NO	NO	YES	NO	YES	YES	NO	[51]	
	3D human extra-embryoids	naïve hPSCs (HENMS condition)	Self organization		YES	YES	YES	YES	YES	YES	YES	YES	NO	[28]	
		RSeT hESCs, trophoblast-like, hypoblast like hPSCs	Self organization	BMP → WNT → NODAL	YES	NO	NO	YES	YES	YES	YES	YES	NO	[29]	
	3D-PASE	hPSCs	Self organization	BMP	YES	NO	NO	NO	YES	NO	NO	NO	YES	YES	[54]
Post-implantation/gastrulation (from 8 dpf)	2D gastruloid	Primed hESCs	BMP	BMP → WNT → NODAL	YES	YES	YES	YES	YES	YES/NO?	NO	NO	YES	YES	[30,55]
	3D gastruloid	Primed hPSCs	WNT (Chiron)	WNT → NODAL	YES	YES	NO	NO	NO	NO	NO	YES	YES*	YES	[32]

their developmental progression [66]. Only most recently, blastoids generated from naïve hPSC reaching early stages of gastrulation have been reported [27]. In this study, 5i/L/A derived naïve hPSCs were aggregated in a simplified blastocyst induction medium to self-assemble by 7 days of culture into cavitating blastoids composed of TE-, EPI and PE-like compartments. Subsequent transfer of these blastoids onto slides coated with a thick layer of extracellular matrix (ECM) supported further development, including evidence of amnion and pro-amniotic cavity formation, substantial expansion of trophoblast and its differentiation into blastoid extravillous trophoblast (EVT) and blastoid syncytiotrophoblasts (STB) by 14 days of culture. Of note, a majority of blastoids in the extended culture expressed TBXT and over 30% showed localized TBXT expression, suggesting symmetry breaking in this model. scRNA-seq analyses at 21 days of culture showed close alignment of this model to the CS7 natural human embryo [3], supporting differentiation of both ME, DE-like cells, and primordial germ cell like (PGCL) cells, yet axial mesoderm markers were not detected [27].

The SCeMs initiated from hPSCs of intermediate pluripotency termed human extra-embryoids (hEEs) that develop organization similar to CS6 embryos and contain amnion and PE-like compartments, form PS-like (TBXT, WNT3A, HES1) and later ME-like (HAND1, MIXL1, MESP1) states [51]. However, DE and TE were not reported in this model. That the amnion-like compartment exhibits high BMP signaling and all EPI-like cells express BMPRI1 supports the notion of a BMP signal emanating from amnion to induce PS (Table 1B). In this system, AVE-like activity was proposed to arise in the PE, initially marked by broad expression of CER1, LEFTY1, GSC, and LEFTY2 with CER1 expression becoming restricted over time. The observation that this restricted CER1 expression in PE mirrored TBXT expression in the overlying EPI implies that AVE-like antagonisms bias TBXT expression and PS induction to the posterior EPI. However, TBXT expression was also observed in SCeMs that did not show any spatial bias in CER1 expression, implying that asymmetric AVE-like activity in the PE might not be necessary for the symmetry breaking in the EPI [51]. In addition to BMP, treatment of hEEs at day 4 with inhibitors of WNT, NODAL, and FGF significantly blocked TBXT expression, consistent with these four pathways being implicated in ME/PS specification in human [51].

Aggregation of human extended PSCs to self-organize into pre- and post-implantation embryo-like structures that exhibit aspects of gastrulation, neurulation and organogenesis has been recently reported [52]. This SCeM, features EPI and hypoblast/PE-like compartments as well as cavitation of the EPI into amnion and EPI embryonic-disc-like structure, without a TE compartment. Formation of TBXT-expressing cells was documented in the prospective posterior end of the embryonic disc/EPI at 8 days of culture. Development of HPGCL, and DE-like, and neural cells were also observed in this model [52].

Representing an approach for producing the human post-implantation embryo model by combining extra-embryonic and embryonic cell types, Weatherbee et al. generated TE- and PE-like cells, by overexpression of transcription factors (TF) in RSeT hESCs of intermediate peri-implantation pluripotency and aggregated them with RSeT hESCs. The aggregated three cell types self-organized to form an EPI-like cluster surrounded by extraembryonic-like cell types resembling post-implantation natural embryos and bypassing a blastocyst-like morphology [29]. Gene expression and chromatin accessibility characterization of cellular composition of the resulting SCeMs at 4–8 days post aggregation revealed differentiation of several EPI derivatives, including amnion-like, HPGCL, extraembryonic mesenchyme-like and ME-like cells (marked by expression of TBXT, MESP1, FOXH1). However, neither differentiation of DE, nor a distinct trophoblast-like cluster were observed. Emergence of amnion- and HPGC-like fates has been attributed largely to BMP signaling, with low levels of NODAL signaling being inferred in the EPI-like domain [29]. In a variation of this approach, Oldak et al. [28] assembled a SCeM using optimized proportions of genetically unmodified naïve hESCs that were stimulated with culture conditions towards embryonic and extraembryonic TE and PE/Extraembryonic mesoderm-like cell types. In the early *in vitro* culture, these integrated SCeMs featured external TE-like compartment marked by CK7 expression surrounding EPI-like with columnar epithelial morphology and PE-like compartments but without a blastocoel cavity. During continued culture, EPI-like compartment formed the amniotic like cavity surrounded by pseudostratified EPI on one side and squamous amniotic epithelium-like on the other with the PE-like compartment forming a Yolk Sack-like cavity. ScRNA-seq interrogation of more advanced SCeMs revealed a cell population expressing markers of EMT and thus nascent PS in the presumed posterior EPI, including TBXT, MIXL1, EOMES, MESP1, and WNT8. Whereas identification of another cluster marked by expression of DKK1, LXH1, and CER1 in PE/Yolk Cell-like compartment supports the existence in this model of AVE-like activity. In addition, this SCeM comprises PGCL cells. However, the current limitation is low efficiency (~1%) with which SCeM of such complex cellular composition and architecture corresponding to *in utero* human embryos at 13–14 dpf (6.5CS) can be generated [28]

Another SCEM of aspects of early gastrulation is the post-implantation amniotic sac embryoid (PASE), in which hESCs cultured with 3D ECM overlay self-organize into an epithelial cyst that features amnion-like and EPI-like epithelia separated by an amniotic-like cavity (Figure 1B) [54,67]. In extended culture of PASE, a PS-like region arises expressing ME but not DE markers. Both the emergence of amnion and subsequently progressive TBXT expression in this system is correlated with self-patterned BMP signaling and BMP signaling inhibition impairs these processes [54]. scRNA-seq profiling of hESC microfluidic PASE and comparison with *in vivo* primate datasets point to a critical role of NODAL signaling in human ME and HPGCL specification [68].

Blastoids and post-implantation SCEMs rely on self-assembly of starting hESCs and intercellular signaling to establish extraembryonic tissues, embryonic polarity, and germ layers. In contrast, in the gastrulation models generated from primed hESCs resembling the pre-gastrulation EPI, germ layers are induced by adding to the culture media components or agonists of the BMP > WNT > NODAL cascade. 2D micropatterned gastruloids were pioneered by Warmflash et al. who seeded primed hESC on 0.5–1 mm discs of ECM under continuous stimulation of BMP4. Instead of heterogenous differentiation of ME, DE, and EC typical of embryoid bodies forming from hESCs in liquid culture [69], 2D micropattern gastruloids differentiate within 48 h into concentric cellular rings of EC-like in the disc's center, surrounded by a PS-like ring of ME and DE-like cells [30]. The most external ring of extraembryonic-like cells was initially identified as TE-like [30,31], but has gene expression pattern similar to both TE and amnion and expresses high levels of BMP4 suggesting it represents amnion [55,70,71]. hPGCL cells are interspersed in the extraembryonic and PS-like regions [55,72]. Despite a global BMP4 application, cells located at the micropattern edge exhibit higher BMP activity as indicated by high levels of pSMAD1 due to apical localization of BMP receptors, compared with the cells in the center that localize the receptors to their basolateral membranes. Furthermore, BMP directly induces the expression of its feedback inhibitor, NOGGIN, and via a reaction-diffusion mechanism establishes a BMP signaling gradient from the edge to the disc's center [73]. Subsequent work demonstrated that BMP signaling induces and maintains waves of WNT and NODAL signaling activity that move toward the colony center, but in a manner inconsistent with a reaction-diffusion model of Turing [31]. BMP and NODAL signaling synergize to control the inward movement of WNT signaling activity. Expression of TBXT is not observed when 2D micropatterns are differentiated in the presence of TGF- β and BMP inhibitors, supporting their essential roles in germ layer induction in this model [30].

The temporal transcriptional dynamics of the signaling pathways' components and the TFs underlying cell fate emergence in 2D micropatterned gastruloids were further analyzed by scRNA-seq at 0, 12, 24, and 48 h [55,70]. These studies support the wave of BMP, WNT, and NODAL signaling in the course of germ layer emergence with transcriptional signature of EC arising first by 12 h, mesendoderm progenitors appearing by 24 h and ME, DE, hPGCL by 48 h. Comparative analysis with scRNA-seq datasets from three mammals as reference (mouse, monkey, and CS7), suggested that 2D micropatterned gastruloids recapitulate temporal emergence and differentiation trajectories of germ layers of *in vivo* gastrulation [70]. The edge ExE-like cells showed strong expression of BMP4 and the negative regulator target gene BAMB1, suggesting signaling activity and a source of BMP ligands similar to that of monkey amnion [6]. Instead, WNT ligands (WNT3, WNT5A), were expressed in the mesendodermal progenitors, ME and EPI, but less in the extraembryonic or EC cell types. Within the NODAL pathway, transcriptome data at 24 and 44 h suggest high NODAL expression in the middle rings comprising EPI-like, ME, and DE. A recent study posits that NODAL, rather than diffusing through embryonic tissues as demonstrated in zebrafish [74], stimulates adjacent cells to transcribe NODAL and therefore regulates NODAL itself in an extremely short-range area [75]. The BMP4-induced 2D micropatterned gastruloids have radial symmetry, they lack PE and likely TE. Moreover, ME-like cells exhibit transcriptomes of somitic, intermediate and lateral plate mesoderm, while axial mesoderm cell types do not form. Of note, axial mesoderm cell types and Spemann–Mangold like activity can be generated in 2D micropatterned hESC cultures stimulated with WNT and ACTIVIN/NODAL signaling [76].

Work by Moris et al. demonstrated the formation of elongating 3D gastruloids. Primed hESCs were pre-treated with a WNT agonist (Chiron) and aggregated in liquid culture with additional stimulation of WNT signaling. Within 24 h, they observed the formation of round aggregates, which elongated by 72–96 h [32]. These 3D gastruloids generate ME, DE, and neuroectoderm-like cell types, but lack extraembryonic cell types or HPGCLs. The arrangement of neuroectoderm-like and ME-like cells at opposite ends of the elongating gastruloids implies a symmetry breaking process and AP axis formation albeit in the absence of extraembryonic tissues. Of note, stimulation of WNT signaling with Chiron could not be substituted with WNT3. Moreover, co-treatment with a BMP inhibitor (LDN192189) impaired the formation of patterned aggregates, but nuclear

localization of SMAD1 reporter was observed in the anterior region, implicating BMP signaling in cardiac development rather than initial germ layer specification. Whereas inhibition of NODAL signaling (SB431542) resulted in aggregates containing cells that co-expressed SOX2 and TBXT, increasing Chiron concentration normalized gastruloid elongation and robust TBXT expression. As the transcriptomic profile of the 3D gastruloids showed similarity to CS8/9 stages of human gastrulation [32], 3D gastruloids model different stages and aspects of gastrulation than 2D gastruloids and the SCEMs that progress through pre-implantation stages.

Primitive streak formation, mesoderm and endoderm internalization and migration *in vivo*

The morphological manifestation of gastrulation in amphibians is the blastopore that takes shape of PS in the mouse and some other amniotes, via which precursors of ME and ED cells internalize beneath the EPI and migrate to their embryonic destinations (Figure 1A) [19]. The molecular hallmark of EMT in PS is nuclear expression of SNAI1 and SNAI2 TFs, transient expression of TBXT, and down-regulation of epithelial characteristics and gene expression, including E-cadherin (CDH1) and ZO1, with a concurrent gain of mesenchymal features such as expression of N-cadherin (CDH2) and motility [77]. In the mouse, PS morphogenesis in the posterior proximal region of the epithelial EPI entails EMT of induced ME and DE precursors; it occurs *in situ* and progresses as a wave towards the distal EPI [78]. However, recent studies posit that in the mouse DE forms via a partial EMT process in which the EMT TF, Snail1, is not required and the cadherin switch is not observed [79]. PS, extending from the posterior/proximal aspect of the EPI to the distal EPI, is evident in the natural human CS7 embryo [3].

Primitive streak formation, mesoderm and endoderm internalization and migration in SCEMs

In the most evolutionarily conserved embryonic gastrulation movement, internalized ME and DE precursors move beneath epiblast and away from the PS in amniotes, blastopore in frogs, and blastoderm margin in zebrafish [19]. ME cells in fish, chick, and mouse move via directed cell migration [80–82]. In murine embryos, Fgf8 is the most highly expressed ligand, and its inactivation partially impairs EMT and movement of ME cells from the PS [83,84]. In human gastrulation, a different FGF ligand might play a key role, as only low levels of FGF8 transcript are observed in ME and DE of 2D gastruloids, which express high levels of FGF17, encoding a related ligand [55,70]. Accordingly, this $FGF8^{low}FGF17^{high}$ signature was reported in ME of CS7 human gastrula [3] and in gastrulating cells of cynomolgus monkey [6]. However, in chick, FGF8 has been proposed to act as chemorepellent to guide ME migration away from the PS [81]. In zebrafish, the migration of internalized ME cells is controlled by Apelin receptor (Aplnr) [85,86] and its ligand Toddler [87]. Interestingly, ME cells in hESC 2D gastruloids [70] express high APLNR levels, as also observed in CS7 human gastrula [3]. However, genetic studies in the mouse argue against a global and essential role of Apela/Apelin/Aplnr signaling in mesoderm migration during gastrulation [88].

A CDH1/CDH2 cadherin switch has been reported in blastoids generated from 5i/L/A naïve hPSCs [27], and at day 4 culture of the hEE embryo model derived from hPSCs of intermediate pluripotency [51]. In the latter model, live imaging revealed that CDH1–CDH2 + SNAI1/2+ cells acquired mesenchymal morphology, appeared to breach the basement membrane and to move in the space between the EPI-like and PE-like layers [51].

In the hPSC PASE model, EMT and cell emigration from the embryonic disc portion occurs. These emigrating cells express nuclear TBXT and SNAI1, membrane-bound CDH2, as well as up-regulated CDX2 and MSX1 TFs, while being negative for FOXA2 and SOX17. This combination suggests the formation of a PS-like structure with migratory ME cells. Of note, this PS-like structure forms in the central region of the embryonic disc and does not expand [54]. Disruption of SNAI1 reduces EMT, formation of the PS-like structure, and cell migration, while not blocking TBXT expression, consistent with the separation of ME induction and morphogenesis. The self-organization of primed hPSCs into an asymmetric cyst of amnion-like squamous epithelium separated from epithelial embryonic disc was proposed to entail endogenously activated high levels of BMP-SMAD signaling in the amniotic epithelium with low levels observed in the embryonic disc [89]. At later stages, high BMP/phospho-SMAD levels are observed in the embryonic disc in the nascent PS-like structure and migrating ME cells [54]. Interestingly, high levels of BMP signaling in posterior PS of human and murine gastrulae might be evolutionarily conserved, as they are also documented in the ventral/posterior region of the zebrafish blastoderm margin/blastopore [90].

hESC 2D micropatterned gastruloids exhibit many cellular and gene expression features of PS, which is ring-shaped in the ME- and DE-like territories (Figure 1B). Cellular rings expressing TBXT up-regulate SNAI, while CDH1 appears to be relocalized from the cell membrane to the cytoplasm and EpCAM epithelial marker is down-regulated [30,55]. Cadherin switching is also seen at the transcriptional level. Moreover, reduced *CDH1* and elevated *CDH2* RNA levels in 2D gastruloids suggest a more conventional EMT of DE in this model of human gastrulation [55]. Expression of components of FGF (including FGFR1), WNT and NODAL pathways in *TBXT*+ cells in 2D gastruloids provides evidence that similar pathways underly EMT in human and mouse. In the PS-like region, several cell layers form in the initially monolayered 2D gastruloid. Furthermore, cells in the bottom layers express SNAI within nuclei, consistent with ME precursors undergoing EMT [30]. Applying the photo-convertible Kik-GR hESC line, migration of cells from the PS-like region towards the center was observed. Whereas, 2D-gastruloids differentiated with WNT3A and ACTIVIN enabled monitoring of the migration of axial mesoderm-like cells, illustrating the potential of this model to study morphogenetic aspects of human gastrulation [91].

The separation of the DE, ME, and EC layers during gastrulation is a fundamental cell sorting event demonstrated by the classic experiments of Holtfreter et al. during which cells from dissociated amphibian gastrulae re-aggregated into three germ layers *in vitro* [92,93]. Whereas such experiments have not been carried out with mammalian gastrulae, 2D micropatterned gastruloids provided an opportunity to test whether human germ layer cells can undergo cell sorting *in vitro*. When differentiated gastruloids were dissociated into single cells and reseeded onto ECM microdiscs, they were migratory and aggregated with similar cell types but segregated from distinct cell types: EC cells segregated from DE and extraembryonic but mixed with ME cells [55]. These observations support that human germ layer cells exhibit evolutionarily conserved sorting behaviors.

3D gastruloids generated from primed hESCs pre-treated with WNT agonists present an intriguing model of gastrulation, as the pre-treated cells express pluripotency markers but also genes associated with ME, DE and PS formation (*TBXT*, *MIXL1*, *EOMES*) and *CDH2* at cell membranes at the time of aggregation [32]. Interestingly, SOX17-positive cells initially emerge throughout the gastruloid, before SOX17 expression becomes confined to the posterior pole. With ME and DE cells already manifesting partial EMT characteristics during aggregation, 3D gastruloids may not model PS formation but reflect behaviors of internalized ME and DE cells. That ME and DE internalization can occur without a full EMT program is well illustrated by emboly in zebrafish, where epiblast is composed largely of mesenchymal cells [9]. It will be of interest to monitor the behaviors of SOX17 DE-like cells initially organized in a salt and pepper fashion and determine the mechanisms via which they congregate.

Convergence & extension (C&E) gastrulation movements

Convergence & extension (C&E) gastrulation movements elongate the germ layers down the anteroposterior embryonic axis, while narrowing them along the mediolateral (dorsoventral) axis. These dramatic morphogenetic movements are achieved by a suite of gastrulation cell behaviors observed in dorsolateral ME, DE, and neuroectodermal tissues, such as directed cell migration, polarized planar and radial cell intercalations, including the famous mediolateral cell intercalation discovered by pioneering studies of Ray Keller in *Xenopus* [19,94,95]. From the hPSC models of gastrulation discussed here, tissue elongation has been observed in 3D gastruloids, whereby the initially round cellular aggregates extend along the nascent anteroposterior axis. However, this process does not appear to be driven by movements of TBXT expressing ME or SOX17 expressing DE cells, which accumulate in the posterior region of the aggregates without apparent extension of these cell populations. The cellular basis of 3D gastruloids' elongation and the underlying signaling mechanisms remain to be investigated. More typical C&E movements likely occur in the embryo models generated from mouse ESCs that form extending axial mesoderm [96]. The absence of axial mesoderm in the current SCeMs is intriguing and the next opportunity for the human SCeM field. It will be important to learn more about the embryonic origins of the axial mesoderm in non-human primate and human embryos whereas transcriptomes of axial mesoderm cells and their progenitors may guide the generation of these cell types in SCeMs.

Posterior body elongation

C&E movements continue to elongate mesodermal and neuroectodermal tissues that arise from the bipotential progenitors in the tailbud. Several hPSC-based models of these processes, as well as segmentation of the presomitic mesoderm have been reported [97,98].

Perspective

The breathtaking progress in deploying hPSCs to model aspects of human development enables investigations of human gastrulation, which has been hidden from experimentation *in utero* and by the 14-day limit on experimentation with human embryos. The repertoire of SCEMs increases daily [18] and these models open doors to investigate induction of germ layers, and the internalization of ME and DE, illuminating their migratory properties. Remarkably, ME- and DE-like cells arise in SCEMs that model pre- and post-implantation development, but also by SCEMs that bypass them. It will be important to stringently compare the three germ layer cell types that form in different models to the growing *in vivo* human and non-human primate gastrulation datasets. Whereas molecular hallmarks of PS are apparent in many SCEMs, PS extension and formation of the Spemann–Mangold organizer at its anterior tip are yet to be modeled in the context of other cell types. The variability and low efficiencies with which some SCEMs are generated make rigorous genetic dissection challenging. The lack in current models of axial mesoderm and of morphological embryonic midline towards which germ layers converge presents an opportunity for SCEM improvements and for advanced models to be devised that more closely recapitulate aspects of human gastrulation.

Summary

- Stem cell-based embryo models (SCEMs) help to understand human gastrulation, a critical developmental process not accessible to experimentation due to technical and ethical limitations.
- Integrated models comprising both embryonic and extraembryonic tissues and non-integrated models lacking some extraembryonic tissues, simulate different aspects of germ layer induction and gastrulation morphogenesis with varied fidelity and efficiency.
- The BMP > WNT > NODAL cascade underlying germ layer induction is supported by experimental evidence in some SCEMs.
- Current evidence from different SCEMs supports epiblast symmetry breaking by signal(s) from primitive endoderm and mesendoderm induction by BMP signaling from amnion.
- Although EMT markers are evident in blastoids, embryoids, and gastruloids, so far ME migration has been observed only in the 3D phase of 2D and 3D gastruloids.
- Current and future SCEMs provide experimental platforms for dissecting the molecular underpinnings of the inductive and morphogenetic processes of human gastrulation and of early pregnancy failure.

Competing Interests

The authors declare that there are no competing interests associated with the manuscript.

Funding

Research on zebrafish gastrulation in the LSK lab is supported by R35 GM118179 grant from NIH/NIGMS and on modeling aspects of human development by the Children Discovery Institute and Washington University School of Medicine in St. Louis.

Authors Contributions

Both authors collaborated on envisioning, writing, editing the text and figures.

Acknowledgements

We thank the members of the Solnica-Krezel laboratory for discussions and Mariana Beltcheva, Rowan Karvas, Thor Theunissen, and Eun-Ja Yoon for comments on the manuscript and discussions.

Abbreviations

AVE, anterior visceral endoderm; CDH1, E-cadherin; CDH2, N-cadherin; dpf, days post fertilization; DE, definitive endoderm; EC, ectoderm; ECM, extracellular matrix; EMT, epithelial-to-mesenchymal transition; EPI, pre-implantation epiblast; ICM, inner cell mass; ME, mesoderm; PASE, post-implantation amniotic sac embryoid; PE, primitive endoderm; PGCL, primordial germ cell like; PS, primitive streak; SCEM, stem cell-based embryo model; TE, trophectoderm; TF, transcription factor.

References

- 1 Jarvis, G.E. (2016) Early embryo mortality in natural human reproduction: what the data say. *F1000Res*, **5**, 2765 <https://doi.org/10.12688/f1000research.8937.2>
- 2 Norwitz, E.R., Schust, D.J. and Fisher, S.J. (2001) Implantation and the survival of early pregnancy. *N. Engl. J. Med.* **345**, 1400–1408 <https://doi.org/10.1056/NEJMra000763>
- 3 Tyser, R.C.V., Mahammadov, E., Nakanoh, S., Vallier, L., Scialdone, A. and Srinivas, S. (2021) Single-cell transcriptomic characterization of a gastrulating human embryo. *Nature* **600**, 285–289 <https://doi.org/10.1038/s41586-021-04158-y>
- 4 Lv, B., An, Q., Zeng, Q., Zhang, X., Lu, P., Wang, Y. et al. (2019) Single-cell RNA sequencing reveals regulatory mechanism for trophoblast cell-fate divergence in human peri-implantation conceptuses. *PLoS Biol.* **17**, e3000187 <https://doi.org/10.1371/journal.pbio.3000187>
- 5 Xiang, L., Yin, Y., Zheng, Y., Ma, Y., Li, Y., Zhao, Z. et al. (2020) A developmental landscape of 3D-cultured human pre-gastrulation embryos. *Nature* **577**, 537–542 <https://doi.org/10.1038/s41586-019-1875-y>
- 6 Ma, H., Zhai, J., Wan, H., Jiang, X., Wang, X., Wang, L. et al. (2019) *In vitro* culture of cynomolgus monkey embryos beyond early gastrulation. *Science* **366**, eaax7890 <https://doi.org/10.1126/science.aax7890>
- 7 Gong, Y., Bai, B., Sun, N., Ci, B., Shao, H., Zhang, T. et al. (2023) Ex utero monkey embryogenesis from blastocyst to early organogenesis. *Cell* **186**, 2092–110.e23 <https://doi.org/10.1016/j.cell.2023.04.020>
- 8 Bergmann, S., Penfold, C.A., Slatery, E., Siriwardena, D., Drummer, C., Clark, S. et al. (2022) Spatial profiling of early primate gastrulation *in utero*. *Nature* **609**, 136–143 <https://doi.org/10.1038/s41586-022-04953-1>
- 9 Solnica-Krezel, L. and Sepich, D.S. (2012) Gastrulation: making and shaping germ layers. *Annu. Rev. Cell Dev. Biol.* **28**, 687–717 <https://doi.org/10.1146/annurev-cellbio-092910-154043>
- 10 Nowotschin, S. and Hadjantonakis, A.K. (2020) Guts and gastrulation: emergence and convergence of endoderm in the mouse embryo. *Curr. Top. Dev. Biol.* **136**, 429–454 <https://doi.org/10.1016/bs.ctdb.2019.11.012>
- 11 Stern, C.D. (2004) Gastrulation. In *From Cells to Embryo* (Stern, C.D., ed.), Cold Spring Harbor Laboratory Press, Cold Spring Harbor, New York
- 12 McClay, D.R., Gross, J.M., Range, R., Peterson, R.E. and Bradham, C. (2004) Sea urchin gastrulation. In *Gastrulation From Cells to Embryo* (Stern, C.D., ed.), pp. 123–137, Cold Spring Harbor Laboratory Press, Cold Spring Harbor, New York
- 13 Stern, C.D. (2004) Gastrulation in the Chick. In *Gastrulation From Cells to Embryo* (Stern, C.D., ed.), pp. 219–232, Cold Spring Harbor, New York, Cold Spring Harbor Laboratory Press
- 14 Ko, C.S. and Martin, A.C. (2020) The cellular and molecular mechanisms that establish the mechanics of Drosophila gastrulation. *Curr. Top. Dev. Biol.* **136**, 141–165 <https://doi.org/10.1016/bs.ctdb.2019.08.003>
- 15 Winklbauer, R. (2020) Mesoderm and endoderm internalization in the *Xenopus* gastrula. *Curr. Top. Dev. Biol.* **136**, 243–270 <https://doi.org/10.1016/bs.ctdb.2019.09.002>
- 16 Winkley, K.M., Kourakis, M.J., DeTomaso, A.W., Veeman, M.T. and Smith, W.C. (2020) Tunicate gastrulation. *Curr. Top. Dev. Biol.* **136**, 219–242 <https://doi.org/10.1016/bs.ctdb.2019.09.001>
- 17 Salehin, N., Knowles, H., Masamsetti, V.P. and Tam, P.P.L. (2022) Mammalian gastrulation: signalling activity and transcriptional regulation of cell lineage differentiation and germ layer formation. *Biochem. Soc. Trans.* **50**, 1619–1631 <https://doi.org/10.1042/bst20220256>
- 18 Moris, N. and Sturmey, R. (2023) In preprints: opportunities to unravel the earliest stages of human development using stem cell-based embryo models. *Development* **150**, dev202295 <https://doi.org/10.1242/dev.202295>
- 19 Solnica-Krezel, L. (2005) Conserved patterns of cell movements during vertebrate gastrulation. *Curr. Biol.* **15**, R213–R228 <https://doi.org/10.1016/j.cub.2005.03.016>
- 20 Wu, E. and Vastenhouw, N. (2020) From mother to embryo: a molecular perspective on zygotic genome activation. *Curr. Top. Dev. Biol.* **140**, 209–254 <https://doi.org/10.1016/bs.ctdb.2020.02.002>
- 21 Goolam, M., Scialdone, A., Graham, S.J.L., Macaulay, I.C., Jedrusik, A., Hupalowska, A. et al. (2016) Heterogeneity in Oct4 and Sox2 targets biases cell fate in 4-cell mouse embryos. *Cell* **165**, 61–74 <https://doi.org/10.1016/j.cell.2016.01.047>
- 22 Lim, H.Y.G., Alvarez, Y.D., Gasnier, M., Wang, Y., Tetlak, P., Bissiere, S. et al. (2020) Keratins are asymmetrically inherited fate determinants in the mammalian embryo. *Nature* **585**, 404–409 <https://doi.org/10.1038/s41586-020-2647-4>
- 23 Hamatani, T., Carter, M.G., Sharov, A.A. and Ko, M.S. (2004) Dynamics of global gene expression changes during mouse preimplantation development. *Dev. Cell* **6**, 117–131 [https://doi.org/10.1016/s1534-5807\(03\)00373-3](https://doi.org/10.1016/s1534-5807(03)00373-3)
- 24 Petropoulos, S., Edsgard, D., Reinius, B., Deng, Q., Panula, S.P., Codeluppi, S. et al. (2016) Single-cell RNA-Seq reveals lineage and X chromosome dynamics in human preimplantation embryos. *Cell* **167**, 285 <https://doi.org/10.1016/j.cell.2016.08.009>
- 25 Rossant, J. and Tam, P.P.L. (2018) Exploring early human embryo development. *Science* **360**, 1075–1076 <https://doi.org/10.1126/science.aas9302>
- 26 Molè, M.A., Weberling, A. and Zernicka-Goetz, M. (2020) Comparative analysis of human and mouse development: from zygote to pre-gastrulation. *Curr. Top. Dev. Biol.* **136**, 113–138 <https://doi.org/10.1016/bs.ctdb.2019.10.002>
- 27 Karvas, R.M., Zemke, J.E., Shahzaib Ali, S., Zhou, C., Dietman, S. and Theunissen, T.W. (2023) 3D-cultured blastoids model human embryogenesis from pre-implantation to early gastrulation stages. *Cell Stem Cell* **30**, 1148–1165.e7 <https://doi.org/10.1016/j.stem.2023.08.005>
- 28 Oldak, B., Wildschutz, E., Bondarenko, V., Comar, M.Y., Zhao, C., Aguilera-Castrejon, A. et al. (2023) Complete human day 14 post-implantation embryo models from naïve ES cells. *Nature* **622**, 562–573 <https://doi.org/10.1038/s41586-023-06604-5>

- 29 Weatherbee, B.A.T., Gantner, C.W., Iwamoto-Stohl, L.K., Daza, R.M., Hamazaki, N., Shendure, J. et al. (2023) Pluripotent stem cell-derived model of the post-implantation human embryo. *Nature* **622**, 584–593 <https://doi.org/10.1038/s41586-023-06368-y>
- 30 Warmflash, A., Sorre, B., Eto, F., Siggia, E.D. and Brivanlou, A.H. (2014) A method to recapitulate early embryonic spatial patterning in human embryonic stem cells. *Nat. Methods* **11**, 847–854 <https://doi.org/10.1038/nmeth.3016>
- 31 Chhabra, S., Liu, L., Goh, R., Kong, X. and Warmflash, A. (2019) Dissecting the dynamics of signaling events in the BMP, WNT, and NODAL cascade during self-organized fate patterning in human gastruloids. *PLoS Biol.* **17**, e3000498 <https://doi.org/10.1371/journal.pbio.3000498>
- 32 Moris, N., Anlas, K., van den Brink, S.C., Alemany, A., Schroder, J., Ghimire, S. et al. (2020) An *in vitro* model of early anteroposterior organization during human development. *Nature* **582**, 410–415 <https://doi.org/10.1038/s41586-020-2383-9>
- 33 Hertig, A.T., Rock, J. and Adams, E.C. (1956) A description of 34 human ova within the first 17 days of development. *Am. J. Anat.* **98**, 435–493 <https://doi.org/10.1002/aja.1000980306>
- 34 Shahbazi, M.N., Jedrusik, A., Vuoristo, S., Recher, G., Hupalowska, A., Bolton, V. et al. (2016) Self-organization of the human embryo in the absence of maternal tissues. *Nat. Cell Biol.* **18**, 700–708 <https://doi.org/10.1038/ncb3347>
- 35 Deglincerti, A., Croft, G.F., Pietila, L.N., Zernicka-Goetz, M., Siggia, E.D. and Brivanlou, A.H. (2016) Self-organization of the *in vitro* attached human embryo. *Nature* **533**, 251–254 <https://doi.org/10.1038/nature17948>
- 36 Bardot, E.S. and Hadjantonakis, A.K. (2020) Mouse gastrulation: coordination of tissue patterning, specification and diversification of cell fate. *Mech. Dev.* **163**, 103617 <https://doi.org/10.1016/j.mod.2020.103617>
- 37 Rossant, J. and Tam, P.P. (2009) Blastocyst lineage formation, early embryonic asymmetries and axis patterning in the mouse. *Development* **136**, 701–713 <https://doi.org/10.1242/dev.017178>
- 38 Kimmel, C.B., Ballard, W.W., Kimmel, S.R., Ullmann, B. and Schilling, T.F. (1995) Stages of embryonic development of the zebrafish. *Dev. Dyn.* **203**, 253–310 <https://doi.org/10.1002/aja.1002030302>
- 39 Ghimire, S., Mantziou, V., Moris, N. and Martinez Arias, A. (2021) Human gastrulation: the embryo and its models. *Dev. Biol.* **474**, 100–108 <https://doi.org/10.1016/j.ydbio.2021.01.006>
- 40 Rivron, N.C., Martinez Arias, A., Pera, M.F., Moris, N. and M'hamdi, H.I. (2023) An ethical framework for human embryology with embryo models. *Cell* **186**, 3548–3557 <https://doi.org/10.1016/j.cell.2023.07.028>
- 41 Weatherbee, B.A.T., Cui, T. and Zernicka-Goetz, M. (2021) Modeling human embryo development with embryonic and extra-embryonic stem cells. *Dev. Biol.* **474**, 91–99 <https://doi.org/10.1016/j.ydbio.2020.12.010>
- 42 Arias, A.M., Marikawa, Y. and Moris, N. (2022) Gastruloids: pluripotent stem cell models of mammalian gastrulation and embryo engineering. *Dev. Biol.* **488**, 35–46 <https://doi.org/10.1016/j.ydbio.2022.05.002>
- 43 Theunissen, T.W. and Jaenisch, R. (2017) Mechanisms of gene regulation in human embryos and pluripotent stem cells. *Development* **144**, 4496–4509 <https://doi.org/10.1242/dev.157404>
- 44 Theunissen, T.W., Powell, B.E., Wang, H., Mitalipova, M., Faddah, D.A., Reddy, J. et al. (2014) Systematic identification of culture conditions for induction and maintenance of naive human pluripotency. *Cell Stem Cell* **15**, 471–487 <https://doi.org/10.1016/j.stem.2014.07.002>
- 45 Takashima, Y., Guo, G., Loos, R., Nichols, J., Ficz, G., Krueger, F. et al. (2014) Resetting transcription factor control circuitry toward ground-state pluripotency in human. *Cell* **158**, 1254–1269 <https://doi.org/10.1016/j.cell.2014.08.029>
- 46 Guo, G., von Meyenn, F., Santos, F., Chen, Y., Reik, W., Bertone, P. et al. (2016) Naive pluripotent stem cells derived directly from isolated cells of the human inner cell mass. *Stem Cell Rep.* **6**, 437–446 <https://doi.org/10.1016/j.stemcr.2016.02.005>
- 47 Dong, C., Belcheva, M., Gontarz, P., Zhang, B., Popli, P., Fischer, L.A. et al. (2020) Derivation of trophoblast stem cells from naive human pluripotent stem cells. *eLife* **9**, e52504 <https://doi.org/10.7554/eLife.52504>
- 48 Guo, G., Stirparo, G.G., Strawbridge, S.E., Spindlow, D., Yang, J., Clarke, J. et al. (2021) Human naive epiblast cells possess unrestricted lineage potential. *Cell Stem Cell* **28**, 1040–56.e6 <https://doi.org/10.1016/j.stem.2021.02.025>
- 49 Linneberg-Agerholm, M., Wong, Y.F., Romero Herrera, J.A., Monteiro, R.S., Anderson, K.G.V. and Brickman, J.M. (2019) Naïve human pluripotent stem cells respond to Wnt, nodal and LIF signalling to produce expandable naïve extra-embryonic endoderm. *Development* **146**, dev180620 <https://doi.org/10.1242/dev.180620>
- 50 Kinoshita, M., Barber, M., Mansfield, W., Cui, Y., Spindlow, D., Stirparo, G.G. et al. (2021) Capture of mouse and human stem cells with features of formative pluripotency. *Cell Stem Cell* **28**, 453–71.e8 <https://doi.org/10.1016/j.stem.2020.11.005>
- 51 Pedroza, M., Gassalolu, S.I., Dias, N., Zhong, L., Hou, T.J., Kretzmer, H. et al. (2023) Self-patterning of human stem cells into post-implantation lineages. *Nature* **622**, 574–583 <https://doi.org/10.1038/s41586-023-06354-4>
- 52 Liu, L., Oura, S., Markham, Z., Hamilton, J.N., Skory, R.M., Li, L. et al. (2023) Modeling post-implantation stages of human development into early organogenesis with stem-cell-derived peri-gastruloids. *Cell* **186**, 3776–92.e16 <https://doi.org/10.1016/j.cell.2023.07.018>
- 53 Hyun, I., Munsie, M., Pera, M.F., Rivron, N.C. and Rossant, J. (2020) Toward guidelines for research on human embryo models formed from stem cells. *Stem Cell Rep.* **14**, 169–174 <https://doi.org/10.1016/j.stemcr.2019.12.008>
- 54 Shao, Y., Taniguchi, K., Townshend, R.F., Miki, T., Gumucio, D.L. and Fu, J. (2017) A pluripotent stem cell-based model for post-implantation human amniotic sac development. *Nat. Commun.* **8**, 208 <https://doi.org/10.1038/s41467-017-00236-w>
- 55 Minn, K.T., Fu, Y.C., He, S., Dietmann, S., George, S.C., Anastasio, M.A. et al. (2020) High-resolution transcriptional and morphogenetic profiling of cells from micropatterned human ESC gastruloid cultures. *eLife* **9**, e59445 <https://doi.org/10.7554/eLife.59445>
- 56 Wang, R., Yang, X., Chen, J., Zhang, L., Griffiths, J.A., Cui, G. et al. (2023) Time space and single-cell resolved tissue lineage trajectories and laterality of body plan at gastrulation. *Nat. Commun.* **14**, 5675 <https://doi.org/10.1038/s41467-023-41482-5>
- 57 Yoon, Y., Huang, T., Tortelote, G.G., Wakamiya, M., Hadjantonakis, A.K., Behringer, R.R. et al. (2015) Extra-embryonic Wnt3 regulates the establishment of the primitive streak in mice. *Dev. Biol.* **403**, 80–88 <https://doi.org/10.1016/j.ydbio.2015.04.008>
- 58 Winnig, G., Blessing, M., Labosky, P.A. and Hogan, B.L. (1995) Bone morphogenetic protein-4 is required for mesoderm formation and patterning in the mouse. *Genes Dev.* **9**, 2105–2116 <https://doi.org/10.1101/gad.9.17.2105>
- 59 Lawson, K.A., Dunn, N.R., Roelen, B.A., Zeinstra, L.M., Davis, A.M., Wright, C.V. et al. (1999) Bmp4 is required for the generation of primordial germ cells in the mouse embryo. *Genes Dev.* **13**, 424–436 <https://doi.org/10.1101/gad.13.4.424>

- 60 Spemann, H. and Mangold, H. (2001) Induction of embryonic primordia by implantation of organizers from a different species. 1923. *Int. J. Dev. Biol.* **45**, 13–38
- 61 De Robertis, E.M., Larrain, J., Oelgeschlager, M. and Wessely, O. (2000) The establishment of Spemann's organizer and patterning of the vertebrate embryo. *Nat. Rev. Genet.* **1**, 171–181 <https://doi.org/10.1038/35042039>
- 62 Yang, R., Goedel, A., Kang, Y., Si, C., Chu, C., Zheng, Y. et al. (2021) Amnion signals are essential for mesoderm formation in primates. *Nat. Commun.* **12**, 5126 <https://doi.org/10.1038/s41467-021-25186-2>
- 63 Mole, M.A., Coorens, T.H.H., Shahbazi, M.N., Weberling, A., Weatherbee, B.A.T., Gantner, C.W. et al. (2021) A single cell characterisation of human embryogenesis identifies pluripotency transitions and putative anterior hypoblast centre. *Nat. Commun.* **12**, 3679 <https://doi.org/10.1038/s41467-021-23758-w>
- 64 Breidenkamp, N., Yang, J., Clarke, J., Stirparo, G.G., von Meyenn, F., Dietmann, S. et al. (2019) Wnt inhibition facilitates RNA-mediated reprogramming of human somatic cells to naive pluripotency. *Stem Cell Rep.* **13**, 1083–1098 <https://doi.org/10.1016/j.stemcr.2019.10.009>
- 65 Rivron, N.C., Frias-Aldegue, J., Vrij, E.J., Boisset, J.C., Korving, J., Vivie, J. et al. (2018) Blastocyst-like structures generated solely from stem cells. *Nature* **557**, 106–111 <https://doi.org/10.1038/s41586-018-0051-0>
- 66 Oura, S., Hamilton, J.N. and Wu, J. (2023) Recent advances in stem cell-based blastocyst models. *Curr. Opin. Genet. Dev.* **81**, 102088 <https://doi.org/10.1016/j.gde.2023.102088>
- 67 Zheng, Y., Xue, X., Shao, Y., Wang, S., Esfahani, S.N., Li, Z. et al. (2019) Controlled modelling of human epiblast and amnion development using stem cells. *Nature* **573**, 421–425 <https://doi.org/10.1038/s41586-019-1535-2>
- 68 Zheng, Y., Yan, R.Z., Sun, S., Kobayashi, M., Xiang, L., Yang, R. et al. (2022) Single-cell analysis of embryoids reveals lineage diversification roadmaps of early human development. *Cell Stem Cell* **29**, 1402–19.e8 <https://doi.org/10.1016/j.stem.2022.08.009>
- 69 ten Berge, D., Koole, W., Fuerer, C., Fish, M., Eroglu, E. and Nusse, R. (2008) Wnt signaling mediates self-organization and axis formation in embryoid bodies. *Cell Stem Cell* **3**, 508–518 <https://doi.org/10.1016/j.stem.2008.09.013>
- 70 Minn, K.T., Dietmann, S., Waye, S.E., Morris, S.A. and Solnica-Krezel, L. (2021) Gene expression dynamics underlying cell fate emergence in 2D micropatterned human embryonic stem cell gastruloids. *Stem Cell Rep.* **16**, 1210–1227 <https://doi.org/10.1016/j.stemcr.2021.03.031>
- 71 Chhabra, S. and Warmflash, A. (2021) BMP-treated human embryonic stem cells transcriptionally resemble amnion cells in the monkey embryo. *Biol. Open* **10**, bio058617 <https://doi.org/10.1242/bio.058617>
- 72 Jo, K., Teague, S., Chen, B., Khan, H.A., Freeburne, E., Li, H. et al. (2022) Efficient differentiation of human primordial germ cells through geometric control reveals a key role for nodal signaling. *eLife* **11**, e72811 <https://doi.org/10.7554/eLife.72811>
- 73 Etoc, F., Metzger, J., Ruze, A., Kirst, C., Yoney, A., Ozair, M.Z. et al. (2016) A balance between secreted inhibitors and edge sensing controls gastruloid self-organization. *Dev. Cell* **39**, 302–315 <https://doi.org/10.1016/j.devcel.2016.09.016>
- 74 Chen, Y. and Schier, A.F. (2001) The zebrafish Nodal signal Squint functions as a morphogen. *Nature* **411**, 607–610 <https://doi.org/10.1038/35079121>
- 75 Liu, L., Nemashkalo, A., Rezende, L., Jung, J.Y., Chhabra, S., Guerra, M.C. et al. (2022) Nodal is a short-range morphogen with activity that spreads through a relay mechanism in human gastruloids. *Nat. Commun.* **13**, 497 <https://doi.org/10.1038/s41467-022-28149-3>
- 76 Martyn, I., Kanno, T.Y., Ruze, A., Siggia, E.D. and Brivanlou, A.H. (2018) Self-organization of a human organizer by combined Wnt and Nodal signalling. *Nature* **558**, 132–135 <https://doi.org/10.1038/s41586-018-0150-y>
- 77 Thiery, J.P., Acloque, H., Huang, R.Y. and Nieto, M.A. (2009) Epithelial-mesenchymal transitions in development and disease. *Cell* **139**, 871–890 <https://doi.org/10.1016/j.cell.2009.11.007>
- 78 Williams, M., Burdsal, C., Periasamy, A., Lewandoski, M. and Sutherland, A. (2012) Mouse primitive streak forms in situ by initiation of epithelial to mesenchymal transition without migration of a cell population. *Dev. Dyn.* **241**, 270–283 <https://doi.org/10.1002/dvdy.23711>
- 79 Scheibner, K., Schirge, S., Burtscher, I., Buttner, M., Sterr, M., Yang, D. et al. (2021) Epithelial cell plasticity drives endoderm formation during gastrulation. *Nat. Cell Biol.* **23**, 692–703 <https://doi.org/10.1038/s41556-021-00694-x>
- 80 Sepich, D.S., Calmelet, C., Kiskowski, M. and Solnica-Krezel, L. (2005) Initiation of convergence and extension movements of lateral mesoderm during zebrafish gastrulation. *Dev. Dyn.* **234**, 279–292 <https://doi.org/10.1002/dvdy.20507>
- 81 Yang, X., Dormann, D., Munsterberg, A.E. and Weijer, C.J. (2002) Cell movement patterns during gastrulation in the chick are controlled by positive and negative chemotaxis mediated by FGF4 and FGF8. *Dev. Cell* **3**, 425–437 [https://doi.org/10.1016/s1534-5807\(02\)00256-3](https://doi.org/10.1016/s1534-5807(02)00256-3)
- 82 McDole, K., Guignard, L., Amat, F., Berger, A., Malandain, G., Royer, L.A. et al. (2018) In toto imaging and reconstruction of post-implantation mouse development at the single-cell level. *Cell* **175**, 859–76.e33 <https://doi.org/10.1016/j.cell.2018.09.031>
- 83 Carver, E.A., Jiang, R., Lan, Y., Oram, K.F. and Gridley, T. (2001) The mouse snail gene encodes a key regulator of the epithelial-mesenchymal transition. *Mol. Cell. Biol.* **21**, 8184–8188 <https://doi.org/10.1128/MCB.21.23.8184-8188.2001>
- 84 Sun, X., Meyers, E.N., Lewandoski, M. and Martin, G.R. (1999) Targeted disruption of Fgf8 causes failure of cell migration in the gastrulating mouse embryo. *Genes Dev.* **13**, 1834–1846 <https://doi.org/10.1101/gad.13.14.1834>
- 85 Zeng, X.X., Wilm, T.P., Sepich, D.S. and Solnica-Krezel, L. (2007) Apelin and its receptor control heart field formation during zebrafish gastrulation. *Dev. Cell* **12**, 391–402 <https://doi.org/10.1016/j.devcel.2007.01.011>
- 86 Scott, I.C., Masri, B., D'Amico, L.A., Jin, S.W., Jungblut, B., Wehman, A.M. et al. (2007) The g protein-coupled receptor agr11b regulates early development of myocardial progenitors. *Dev. Cell* **12**, 403–413 <https://doi.org/10.1016/j.devcel.2007.01.012>
- 87 Stock, J., Kazmar, T., Schlumm, F., Hannezo, E. and Pauli, A. (2022) A self-generated Toddler gradient guides mesodermal cell migration. *Sci. Adv.* **8**, eadd2488 <https://doi.org/10.1126/sciadv.add2488>
- 88 Freyer, L., Hsu, C.W., Nowotschin, S., Pauli, A., Ishida, J., Kuba, K. et al. (2017) Loss of apela peptide in mice causes low penetrance embryonic lethality and defects in early mesodermal derivatives. *Cell Rep.* **20**, 2116–2130 <https://doi.org/10.1016/j.celrep.2017.08.014>
- 89 Shao, Y., Taniguchi, K., Gurdziel, K., Townshend, R.F., Xue, X., Yong, K.M.A. et al. (2017) Self-organized amniogenesis by human pluripotent stem cells in a biomimetic implantation-like niche. *Nat. Mater.* **16**, 419–425 <https://doi.org/10.1038/nmat4829>
- 90 Zinski, J., Bu, Y., Wang, X., Dou, W., Umluis, D. and Mullins, M.C. (2017) Systems biology derived source-sink mechanism of BMP gradient formation. *eLife* **6**, e22199 <https://doi.org/10.7554/eLife.22199>
- 91 Martyn, I., Siggia, E.D. and Brivanlou, A.H. (2019) Mapping cell migrations and fates in a gastruloid model to the human primitive streak. *Development* **146**, dev179564 <https://doi.org/10.1242/dev.179564>

- 92 Steinberg, M.S. and Gilbert, S.F. (2004) Townes and Holtfreter (1955): directed movements and selective adhesion of embryonic amphibian cells. *J. Exp. Zool. A Comp. Exp. Biol.* **301**, 701–706 <https://doi.org/10.1002/jez.a.114>
- 93 Townes, P.L. and Holtfreter, J. (1955) Directed movements and selective adhesion of embryonic amphibian cells. *J. Exp. Zool.* **128**, 53–120 <https://doi.org/10.1002/jez.1401280105>
- 94 Shih, J. and Keller, R. (1992) Cell motility driving mediolateral intercalation in explants of *Xenopus laevis*. *Development* **116**, 901–914 <https://doi.org/10.1242/dev.116.4.901>
- 95 Keller, R. (2002) Shaping the vertebrate body plan by polarized embryonic cell movements. *Science* **298**, 1950–1954 <https://doi.org/10.1126/science.1079478>
- 96 Xu, P.F., Borges, R.M., Fillatre, J., de Oliveira-Melo, M., Cheng, T., Thisse, B. et al. (2021) Construction of a mammalian embryo model from stem cells organized by a morphogen signalling centre. *Nat. Commun.* **12**, 3277 <https://doi.org/10.1038/s41467-021-23653-4>
- 97 Budjan, C., Liu, S., Ranga, A., Gayen, S., Pourquié, O. and Hormoz, S. (2022) Paraxial mesoderm organoids model development of human somites. *eLife* **11**, e68925 <https://doi.org/10.7554/eLife.68925>
- 98 Miao, Y., Djeflal, Y., De Simone, A., Zhu, K., Lee, J.G., Lu, Z. et al. (2023) Reconstruction and deconstruction of human somitogenesis *in vitro*. *Nature* **614**, 500–508 <https://doi.org/10.1038/s41586-022-05655-4>